CHARACTERIZATION OF ELECTRICAL DISCHARGES ON TEFLON DIELECTRICS USED AS SPACECRAFT THERMAL CONTROL SURFACES*

E. J. Yadlowsky, R. C. Hazelton and R. J. Churchill
Colorado State University†

SUMMARY

The dual effects of system degradation and reduced life of synchronous-orbit satellites as a result of differential spacecraft charging underscore the need for a clearer understanding of the prevailing electrical discharge phenomena.

In a laboratory simulation, measurements are made of electrical discharge current, surface voltage, emitted particle fluxes, and photo-emission associated with discharge events on electron beam irradiated silver-backed Teflon samples. Sample surface damage has been examined with optical and electron beam microscopes. The results are suggestive of a model in which the entire sample surface is discharged by lateral sub-surface currents flowing from a charge deposition layer through a localized discharge channel to the back surface of the sample. The associated return current pulse appears to have a duration which may be a signature by which different discharge processes may be characterized.

INTRODUCTION

In situ measurements on synchronous-orbit satellites during magnetic substorm activity have indicated that the associated electrical discharges result from differential charging of satellite surfaces by fluxes of high energy electrons (≳ 20 KeV). The task of ameliorating the effect of spacecraft charging on satellite performance requires a clear understanding of the charging and discharging phenomena. In particular, the system parameters which determine the electrical breakdown threshold, the particles emitted and electrical currents associated with the breakdown must be understood. This information would facilitate the development of techniques to alleviate electrical stresses on satellite components and of models to predict locations on the satellite of minimum electromagnetic interference where sensitive instrumentation could be located.

---

*Sponsored by NASA GRANT NSG-3145
†The authors are now at Kollmorgen Corporation, 501 First Street, Radford, Virginia

The research program described here deals with the characteristics of breakdown events on silver-backed Teflon samples irradiated by a monoenergetic beam of electrons under conditions where the sample edges have been shielded from direct irradiation by the electron beam. The dependence of the minimum breakdown voltage on sample thickness and irradiation history was determined. The additional evaluation included the dependence on sample area and breakdown voltage of the transient currents associated with the discharges, the energy and angular distribution of the particles emitted, and the temporal characteristics of the emitted light. Surface damage resulting from discharge events was studied using optical and scanning electron beam microscopes.

The results indicate that puncture breakdowns through the sample are prevalent, that the sample is discharged by lateral surface currents which flow beneath the sample surface, and that plasma effects are important in the discharge process. Further, the discharges are observed to fit two distinct groups with the time duration of the return current pulse being a convenient distinguishing characteristic.

In the remainder of the paper, the experimental system is discussed briefly. This is followed by a presentation of the experimental technique and the measurements obtained. A discussion of results and a conclusion section complete the paper.

EXPERIMENTAL SYSTEM

The spacecraft charging phenomenon is simulated in a vacuum chamber by irradiating a dielectric target with a high-energy electron beam. It is convenient to discuss the total system relative to the schematic diagram shown in figure 1.

The simulation chamber consists of a 30 cm diameter cylindrical glass tube about 1 meter in length. Four cylindrical ports 15 cm in diameter located at the central section of the tube provide outlets for vacuum ports, introduction of electrical and photographic measurement systems and the installation of target assemblies. The electron beam gun is located at one end of the 30 cm diameter cylinder and generates an axial electron beam to the centrally located target area. Base pressures of 10^{-7} Torr are possible using a 10 cm diameter oil diffusion pump system.

To simulate the spacecraft charging, the dielectric targets are bombarded with a mono-energetic divergent electron beam having an acceleration potential from 0 to 34 kV and a beam current density at the target location of 0-5 nA/cm^2. Uniformity of the electron beam over the target area is about 25% for a 10 cm diameter target located 50 cm from the electron beam gun.

The silver-backed dielectrics used in the irradiation process are mounted on various target assemblies at the center of the four-port region of the simulation chamber so as to have the dielectric front surface of the target at an angle of 50° to the axis of the electron beam. The sample is

supported by an annular aluminum ring providing electrical contact to the silver-backed Teflon sample through conducting paint. The entire sample holder is placed within, but electrically insulated from, a grounded enclosure containing an aperture through which the sample is irradiated. By means of this arrangement, the sample edges are not irradiated directly by the electron beam thus facilitating breakdown studies not dominated by edge effects. The aperture opening can be varied from 2.5 cm to 8 cm dia. by controlling the opening of an adjustable iris mounted on the sample enclosure. The control linkage is brought through the vacuum wall to facilitate the study of discharge properties which depend on the surface area irradiated. The front surface of the sample is visible for inspection and photographic measurements.

The electron beam voltage required to initiate a breakdown is determined by irradiating the sample to nearly steady state conditions with successively larger accelerating beam voltages until a discharge occurs.

The transient current that flows to the silver backing on the sample during a discharge event is measured by a Tektronix CT-1 current probe clipped on the lead connecting the silver backing to ground potential.

A system of mirrors and viewing ports permits time-integrated photographs of the self-luminous electrical discharges to be taken. The resultant photographs of the discharge path along the sample surface and the central site of the discharge are correlated with scanning electron microscope studies of material damage.

Charged particle measurements are made using a biased Faraday cup and a retarding potential analyzer (RPA), both of which are illustrated in figure 2. The Faraday cup consists of a shielded collector which can be biased to collect either positive or negative particles through a grid aperture of 2.5 cm. The output current of the collector is shunted to ground through a 50 ohm load and the resulting voltage measured with a Tektronix 556 oscilloscope.

The retarding potential analyzer used for the measurement of emitted particles consists of a particle collector plate and two independently biasable grids enclosed in a grounded shield having an input aperture of 1.2 cm. For the measurement of positive particles the collector is biased at -9 V to capture the positive particles which pass through the grids. Grid G2, the suppressor grid, is biased at -800 V to prevent secondary electron emission from the collector surface which could be erroneously interpreted as positive particles. The first grid is then biased positively to define a threshold energy for the incoming particles. By varying the bias on the first grid the energy spectrum of the incoming ions can be measured.

The output of the collector is measured in a manner identical to that used with the Faraday cup. A temporally resolved particle flux is thereby derived and particle transit times and total particle emissions are determined. Similar measurements are made for negative particles with the collector biased to + 9 V, the second grid grounded, and the first grid biased negatively. In all cases the amplitudes of the incident particle fluxes are derived

by multiplying the measured signal by the weighting factor of 1.8 to account for grid attenuation. The distribution of particle energies is obtained from the measured dependence of collector current on retarding grid voltage by graphical differentiation.

For the angular measurements presented herein, the probes were positioned as shown in figure 3. The sample is tilted $\sim 40^{\circ}$ to the beam axis to allow observation of normally emitted particles free from detector interference with the beam. The Faraday cup is set at a fixed angle of 40° below the horizontal plane, 9.5 cm from the sample surface. The RPA is located about 15 cm from the sample center and is free to pivot some 70° about the sample center line. The entrance aperture of the RPA subtends an angle of 3° with respect to a point on the target surface.

A high energy retarding potential analyzer (HERPA) was designed to provide a retarding potential of up to 11 kV. The HERPA is positioned 9.2 cm from the sample surface and has an aperture of 5.6 cm. Measurements are made in a fashion identical to those of the RPA.

The temporal characteristics of the light emitted during an electrical breakdown were recorded using an optical system consisting of an f/2 lens collection system, fiber optics to transmit the light signal through the wall of the vacuum chamber and a photomultiplier to detect the signal.

EXPERIMENTAL RESULTS

In order to provide a coherent and consistent picture of the electrical discharge process on the dielectric samples, measurements have been made of minimum breakdown voltage, material damage, return currents, particle emission and photo-emission from the sample surface.

Breakdown Voltage

The breakdown voltage was measured for previously unirradiated samples of thickness 25, 50, 75 and 125 μ (1,2,3 and 5 mil) silver-backed Teflon. Since a method of direct measurement of surface potential was unavailable, the surface potentials at breakdown were inferred from the measured electron beam voltage. Work by Stevens (private communication) indicates that the measured surface potential is 1.8 kV less than the beam voltage. The thresholds are plotted against sample thickness in figure 4 and demonstrate a reasonably linear correlation between thickness and breakdown voltage. The history of the breakdown occurring on a single 75 μ sample (fig. 5) demonstrates a wide variation in the breakdown voltage. For the particular example shown the initial breakdown voltage is 26 kV decreasing to 14 kV after 20 breakdowns. It is noteworthy that the breakdown voltage does not stabilize at any particular value.

Material Damage

Material damage on the irradiated dielectric surface following an electrical discharge has been studied using an optical microscope and a scanning electron beam microscope (SEM). The optical microscope reveals information about sub-surface damage as well as surface damage whereas the SEM is used for high resolution surface studies. The photographs in figure 6 reveal a hole through the dielectric material to the grounded silver backing resulting from the discharge current flow. In addition, this microscopic investigation reveals the existence of filamentary surface tracks which terminate at the holes as in figures 6a and 6b. These material damage tracks are similar in form and appearance to luminous Lichtenberg streamers observed on the surface during the discharge, although no direct comparison has been made. The tracks in the Teflon appear to be the results of currents which flow through the Teflon parallel to the surface during the discharge of the sample. Ionization and recombination in the current channels are accompanied by light emission which gives rise to the luminous Lichtenberg patterns. The process of discharging the sample by currents flowing underneath the sample surface is consistent with puncture sites where filamentary material damage has occurred as in figures 6a and 6b. In figure 6c, a current filament is seen to surface a number of times before reaching the main discharge channel.

The microphotographs of the discharge sites dramatically demonstrate the material damage resulting from the discharges on the sample. It is evident that the energy in the current channel is sufficient to rupture the channel as in figure 6b and to eject molten Teflon from the puncture site. In addition, there is appreciable silver loss from the grounded silver backing as seen in figure 6d as well as extensive melting and ejection of material from the discharge sites.

Return Current

Return currents to the sample were measured during a discharge with a Tektronix CT-1 current probe and a Tektronix oscilloscope. Since the probe was installed outside of the vacuum system, a shielded cable leading from the sample to the probe was terminated in its characteristic impedance (50 ohms) so as to minimize reflections.

From numerous observations of the return current associated with a breakdown, two distinct categories of pulses have been identified. The first is characterized by a long duration pulse of 200 to 400 ns, while the second is represented by a short pulse of 20 ns duration. These two time scales appear to relate to different discharge processes and are discussed in the next section.

In addition, the total charge in the return current pulses was determined by integrating the recorded current traces. Figure 7 illustrates the relationship between this charge and the irradiated area of the sample

surface. Although there are large shot-to-shot variations in total charge a generally linear relationship exists implying that the entire sample surface is discharged during a given event.

Particle Emission

Using the particle collecting probes (Faraday cup, RPA, HERPA), the charge, energy, and angular distribution of the particles emitted during a discharge were determined. Figure 8 shows two traces from the Faraday cup with the bias first set to collect negative particles (8a) and then to collect positive particles (8b). The time history of negative particles includes an early electron spike followed by a longer electron pulse. The early pulse is present in all breakdowns while the later pulse is intermittent.

The maximum retarding potential (3 kV) of the RPA was not sufficient to reduce significantly the amplitude of the early spike. Therefore, a high energy retarding potential analyzer (HERPA) was designed and tested to 11 kV. Using this probe the energy of the electrons in the early spike was found to be in the range of 5-7 keV.

The later pulse of electrons exhibited energies less than the threshold sensitivity of the RPA ($\simeq$1eV). Coincident with the late electron pulse is a pulse of positive particles as shown in figure 8b. Using the RPA, the particle flux was measured as a function of the retarding potential as shown in figure 9. From figure 9 the energy of the positive particles is estimated to be 70 eV. The total number of electrons and positive particles is of the same magnitude. The coincidence of arrival times, the equality of particle number and the relative energies of the positive and negative particles all imply that the late pulse leaving the sample constitutes a plasma.

Figure 10 shows the total number of early electrons as a function of the irradiated area of the sample. As with the return current, the number of emitted particles is linearly related to the area of the sample.

Light Emission

Light emission during electrical discharge was measured in conjunction with the return current pulse. The experimental data clearly shows that the emitted light signals follow closely upon the return current. It may also be observed that the emitted light persists for 100 ns beyond the point at which the return current pulse has decreased to zero. It should also be noted that the amplitude of the light emission during the short return current pulse is four times as large as that occurring during the long duration return current pulse.

DISCUSSION OF RESULTS

A consideration of the measurements presented provides a physical picture of the general process by which the sample surface is discharged. The interrelationship of these measurements leading to a cataloging of different discharge processes is presented in this section.

The dependence of the minimum breakdown voltage on the shielding of the sample edges, on sample thickness, and on the previous history of discharges on the sample provides insight into the material characteristics which govern the breakdown voltage.

The dramatic increase in the minimum breakdown voltage from 15 kV to 32 kV for a 125 μ (5 mil) sample when the sample edges are shielded from irradiation indicates that bulk properties of the sample control the breakdown threshold once surface effects associated with sample edges are eliminated. The slope of the straight line in figure 4 yields a breakdown strength for the bulk material of 2.6×10^6 V/cm (6.5 kV/mil) which is in good agreement with the manufacturers' value of 1.8×10^6 V/cm (ref. 1) for a 75 μ sample. Preexisting defects are expected to depress the breakdown voltage from the ideal value. This can be seen in figure 5 where the value for the first 20 discharges is decreasing on the average. The discharges can also alter the material properties to increase the breakdown voltage as seen by the non-monotonic variation.

The sub-surface crazing together with the surface cracks are similar in form to the luminous Lichtenberg patterns and are in close agreement with the observation of others (Crutcher, private communication). The fissures are evidence for current channels formed by vaporization and ionization of the dielectric material. They imply that the surface is discharged by lateral currents flowing beneath the surface and indicate the extent of the region discharged.

All of the return current pulses represent a unidirectional flow of electrons from ground to the silver backing on the sample, in agreement with the observation of Berkopec *et al.* (ref. 2) The majority of the return current pulses could be classified as short (≈ 20 ns half-width) or long (200-400 ns) with a few scattered values of 90-120 ns. The trend in figure 5 is for the short pulses to be associated with peak values in the breakdown voltage and long pulses to be associated with decreasing or minimum values in threshold voltage. The total charge in the pulse appears to depend on the irradiated area for the long pulse but not the short pulse. Although there is scatter in the data, the relatively straight line through the maximum values of charge flow for long pulses in figure 7 indicates that the entire sample surface irradiated is being discharged under the conditions studied. Stevens (private communication) has observed both partial and total discharges of the sample which could account for some of the scatter in the data. This classification of return current pulses as to short or long pulses provides a convenient method for distinguishing between different discharge phenomena.

The emission of particles from the surface was studied to determine the origin of the return current pulse. The initial burst of high energy electrons accounts for the polarity of the return current pulse. The energy of the particles is in the range of 5-7 keV for the duration of the pulse. Since the time of flight for these electrons (20 ns) is much less than the duration of emission, the pulse length of the high energy electron emission appears to be representative of the sample discharge time.

Both the short and the long duration emissions of high energy electrons occur simultaneously with the corresponding return current pulse. The two-fold difference in duration for the particle emission is a factor of 10 less than the difference in the return current case. The results tend to support the observations of Nanevicz and Adamo (ref. 3) and Gross *et al.* (ref. 4) that electrons are emitted during a discharge.

The later pulse consisting of positive ions and electrons was observed only when the return current pulse was short. The magnitude and duration of the positive and negative particle signals indicate that the particles are emitted as a near neutral plasma. An insight into the nature of the pulse is obtained from a consideration of the particle energies. The results shown in figure 9 indicate that the ions are emitted with a minimum energy of 30 eV. Another estimate of the particle energies can be obtained by determining the time of arrival of the particles at the collector from the temporal evolution of the collector signal. From the transit time and known sample-to-detector distance the velocity, and hence, kinetic energy can be determined. The results again show that all the particle energies exceed a minimum value. By equating the minimum energies, an estimate of the positive ion mass can be found if the ion is assumed to be singly ionized. The value of 13.3 amu so obtained is sufficiently close to the atomic weight of carbon 12 to encourage a tentative identification of the later positive ion peaks as due to singly ionized carbon, although the data is not sufficiently definitive to rule out fluorine.

An estimate of the currents flowing on the sample surface can be obtained by dividing the total charge of the 75 μ thick sample charged to 24 kV by the time given by the duration of the high energy electron burst. This value (300 A) can account for the vaporization and ionization required to produce a plasma. The presence of the plasma pulse in turn accounts for the light emission during the discharge as well as the sub-surface cracks and fissures on the sample.

CONCLUSION

The somewhat random variation in the measured parameters in this study indicates the complex and changing nature of the electrical discharges. Therefore, the need to develop a realistic model becomes readily evident.

The experiments indicate that puncture discharges occur when the Teflon sample edges are shielded from direct irradiation by the electron beam. Under

these conditions the surface voltage of an irradiated sample increases until the electric field strength within the sample, possibly at a material defect, exceeds the dielectric strength of the material, thereby initiating a breakdown through the sample with the grounded silver backing, serving as one electrode. Apparently the entire sample surface can be discharged by lateral currents flowing beneath the surface. Material damage in the form of fissures and cracks results from these currents. Correlation of light emission and return current measurements indicates plasma formation takes place during the initial stages of the breakdown process. The plasma formed provides the necessary conducting paths for discharging the sample. The burst of high energy electrons accounts for the polarity of the return current and provides a measure of the sample discharge time.

Another significant feature is the duration of the return current pulse which is an easily measured parameter to distinguish between two different discharge processes. When a long duration return current pulse is observed, the following discharge characteristics are also present: a) particle emission consists of a relatively long burst of high energy electrons, b) the total charge in the return current pulse is proportional to the irradiated area of the sample, and c) the light emission indicates a low-amplitude, long-duration pulse. For a short duration return current pulse the following discharge characteristics are observed: a) particle emission consists of a relatively short burst of high energy electrons followed by a later near-neutral pulse consisting of positive ions and electrons, b) the total charge in the return current pulse is independent of irradiated sample area, and c) the light emission is a large amplitude short pulse.

If the experimental results are sorted according to the time duration of the return current pulse, a meaningful identification of the discharge characteristics emerges. Correlation of experimental parameters thereby generates signatures useful in the delineation of the various discharge processes.

REFERENCES

1. DuPont Technical Information Bulletin T-4D

2. Berkopec, F. D.; Stevens, N. J.; and Sturman, J. C.: The LeRC Substorm Simulation Facility. USAF/NASA Spacecraft Charging Technology Conference, Colorado Springs, Oct. 27-29, 1976.

3. Nanevicz, N. E. and Adamo, R. C.: Malter Discharges as a Possible Mechanism Responsible for Noise Pulses Observed on Synchronous-Orbit Satellites. Progress in Astronautics and Aeronautics, vol. 47, A. Rosen, ed., Cambridge MIT Press, 1976, pp. 247-261.

4. Gross, B.; Sessler, G. M.; and West J. E.: Radiation Hardening and Pressure - Actuated Charge Release of Electron-Irradiated Teflon Electrets. App. Phys. Lett., vol. 24, no. 8, 1974, pp. 351-353.

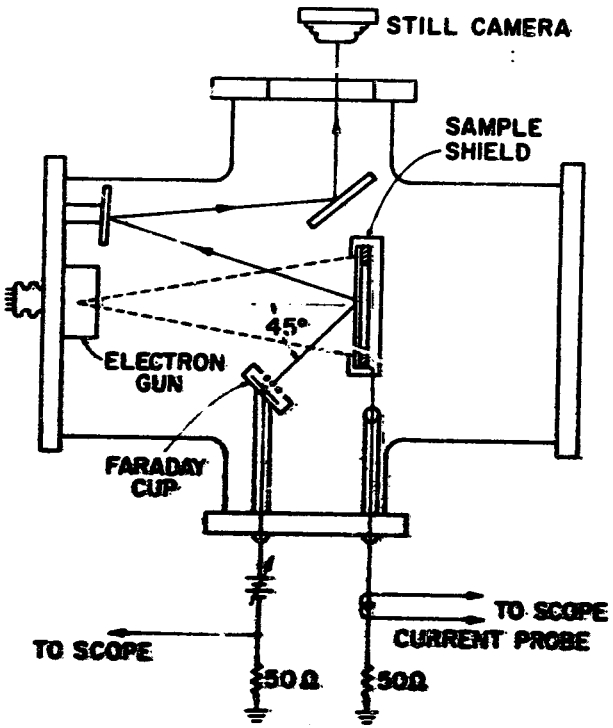

FIGURE 1. SPACECRAFT CHARGING SIMULATOR AND MEASUREMENT SYSTEM.

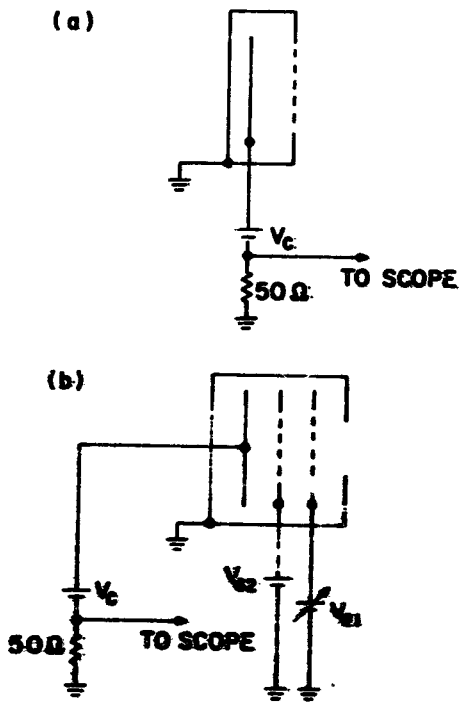

FIGURE 2. CHARGED PARTICLE DETECTORS:
(a) FARADAY CUP
(b) RETARDING POTENTIAL ANALYZER

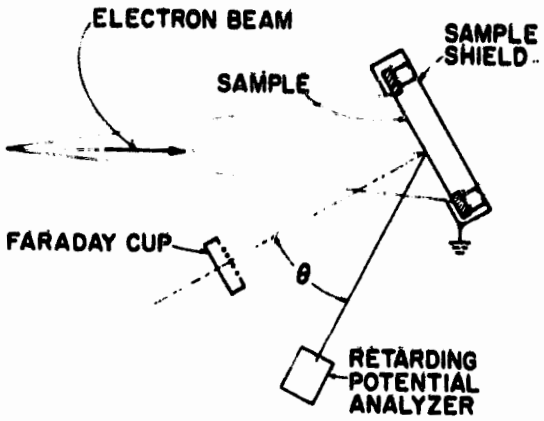

FIGURE 3. ANGULAR DISTRIBUTION MEASUREMENT SYSTEM (RELATIVE ORIENTATION OF DIELECTRIC SAMPLE, ELECTRON BEAM AND CHARGED PARTICLE DETECTORS).

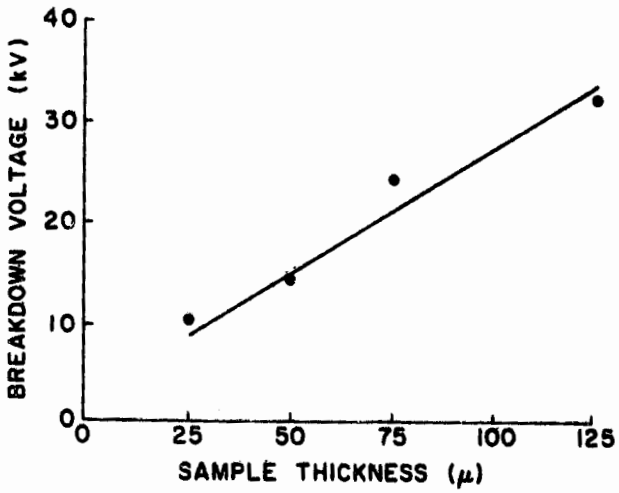

FIGURE 4. ELECTRICAL BREAKDOWN OF SILVER-BACKED TEFLON SAMPLES.

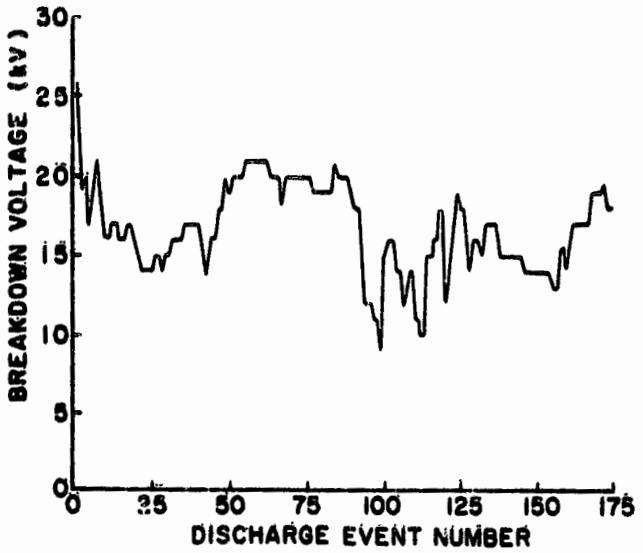

FIGURE 5. HISTORY OF BREAKDOWN VOLTAGE FOR 75μ SILVER-BACKED TEFLON SAMPLE.

(a) OPTICAL MICROGRAPH SHOWING SUBSURFACE FILAMENTARY STRUCTURE. (75 X)

(b) SCANNING ELECTRON MICROGRAPH OF BREAKDOWN SITE SHOWN IN 6a. (190 X)

(c) SCANNING ELECTRON MICROGRAPH OF FILAMENTARY STRUCTURE NEAR BREAKDOWN SITE SHOWN IN 6a. (225 X)

(d) SCANNING ELECTRON MICROGRAPH OF DAMAGE TO SILVER SIDE. (225 X)

FIGURE 6. 75 μ SILVER-BACKED TEFLON SAMPLE IRRADIATED AT 26 kV WITH A BEAM CURRENT DENSITY OF ~ 1 nA/cm².

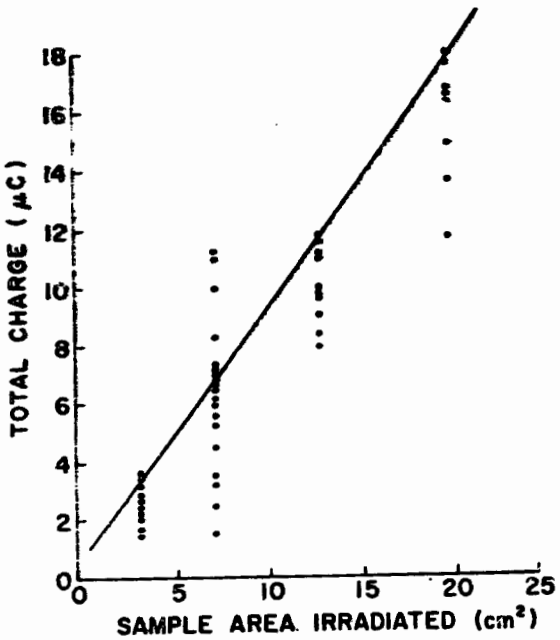

FIGURE 7. CHARGE CONTAINED IN RETURN CURRENT PULSE FOR VARIOUS SAMPLE AREAS IRRADIATED.

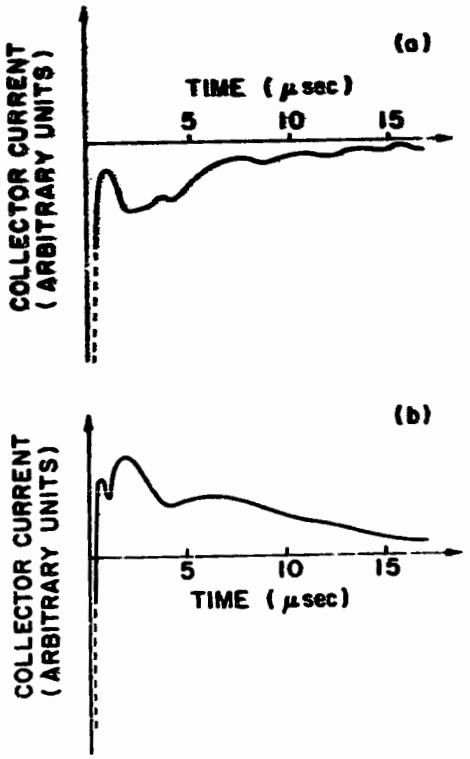

FIGURE 8. OSCILLOSCOPE TRACES OF FARADAY CUP CURRENT:
(a) FARADAY CUP BIASED TO COLLECT NEGATIVE PARTICLES
(b) FARADAY CUP BIASED TO COLLECT POSITIVE PARTICLES.

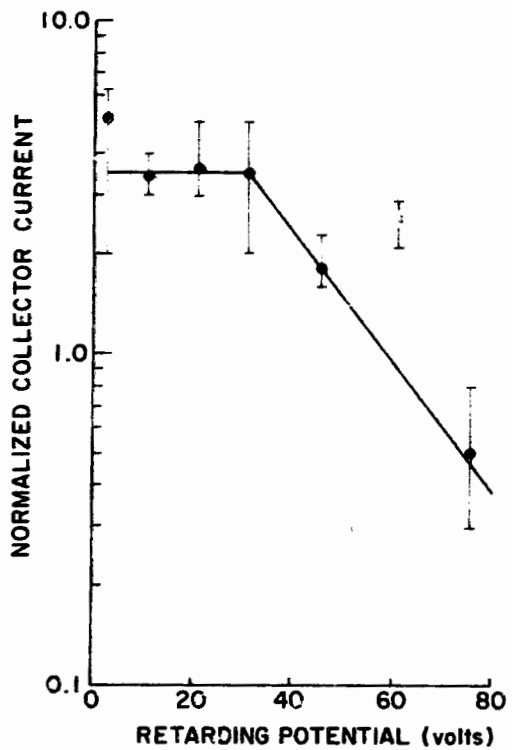

FIGURE 9. ENERGY DISTRIBUTION OF POSITIVE IONS MEASURED WITH THE RETARDING POTENTIAL ANALYZER.

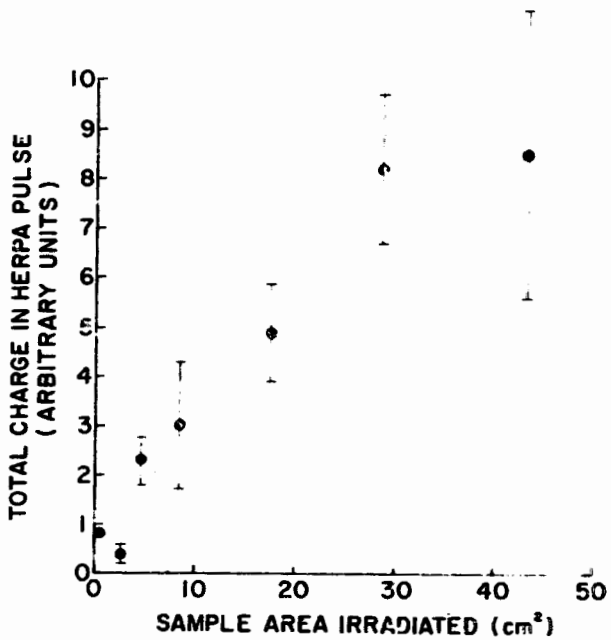

FIGURE 10. CHARGE CONTAINED IN EARLY ELECTRON PULSE FOR VARIOUS SAMPLE AREAS IRRADIATED.